Universitatea "Babeș-Bolyai"
Facultatea de Fizică
Școala Doctorală de Fizică

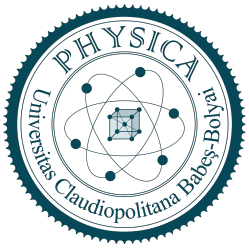

Doctoral Thesis

Andrei Butuza

Scientific coordinator
Prof. dr. Grigore Damian

Cluj-Napoca
2025

Universitatea "Babeș-Bolyai"
Facultatea de Fizică
Școala Doctorală de Fizică

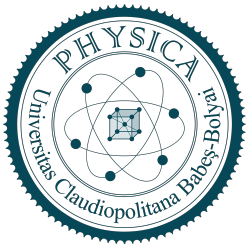

DOCTORAL THESIS

Obtaining important observables of interest in the case of the nuclear fission of Rn and Ra

Andrei BUTUZA

Scientific coordinator
Prof. dr. Grigore DAMIAN

Cluj-Napoca
2025

Contents

1 Introduction

The process of nuclear fission has been a topic of interest for experimentalists and theoreticians alike since the discovery of the process in 1938. The process is not yet fully explained. There is plenty of experimental data which covers the process but the theoretical models need to improve steadily to provide a clear picture of the process. The Liquid Drop Model (LDM) is a model that was greatly used, though it presents some limitations in regard to explaining the permanent deformations of nuclei in ground state or the asymmetric mass distributions in the fission of actinides. Such limitations can be overcome by considering single particle models. As such, a macroscopic-microscopic method stands out. In such cases, a demand appears for a refined calculation of potential energy surfaces as all observables of interest are sensitive to them.

This current work aims to describe and predict the characteristics of the binary decay products resulting from the process of induced fission, particularly. To this end, the dinuclear system model (DNS) has been implemented and used, which is an improved version of a scission point model. The critical component of the model is the calculation of the potential energy surfaces which are dependent on the mass and charge of the fragments as well as deformations. Other features of interest of the model are the handling of energy in the system between some inter-fragment interaction potentials and in the case of each fragment, the description of its macroscopic energy as well as microscopic shell corrections. The model will determine excitation energies which provide the system temperature, both being of import in the calculation of various distributions.

The thesis is structured in the following manner, after the introduction will come the first chapter which will cover the theory of the model in detail and different components are introduced and explained. The second chapter will cover the charge distribution and total kinetic energy results obtained

in the case of the radon and radium nuclei studied. Here are presented also other distributions that help interpret the obtained results. The third chapter covers the neutron multiplicities and discussion related to peculiarities in some isotopes.

2 Model Description

2.1 Dinuclear system

On the fission path, there are two particular points of interest, the saddle point and the scission point. The "saddle point" is defined as the point where the rate of change for the Coulomb energy is equal to the rate of change of surface energy. The "scission point" is the point where the nascent fragments are individualized, having no overlap in their nuclear densities, but still remain within the effective range of their mutual nuclear forces. With the appearance of the two-center model, we can calculate a single particle structure. The spectra for a scission configuration corresponding to a single particle is similar enough to the single particle levels of the newly created individual fragments that we make a powerful observation. This observation suggests that a fragment is mostly indifferent of the way in which it was formed and its properties are irrespective of the fission event.

The dinuclear system (DNS) is built upon this result and it depicts the scission configuration as two individualized fragment nuclei interacting with one another via a repulsive Coulomb interaction and an attractive nuclear one. The DNS system features some interesting properties. One of these properties is that the fission fragments are individualized having no overlap in their nuclear densities. Another property is that the system is relatively unstable and can evolve in a couple ways: the fragments might exchange nucleons that are weakly bound, the fragments might drift away from one another, due to the nature of the potentials affecting them, the fragments might deform under the attractive and repulsive potentials and finally, the system might start to rotate if it suffers a collision with a heavy ion. The potential energy would drive the system to evolve in all of these dimensions. The last property of interest would be that the evolution of the system in regards to mass and charge numbers is of a statistical nature as we are

considered to be in thermal equilibrium.

2.2 Potential energy

The total energy of the system can be split into three parts: the binding energies of each fragment, the interaction potential and the rotational energy. The last part is not covered in this work.

2.2.1 Geometrical aspects

We consider the system as two axially symmetric prolate deformed ellipsoids situated at a distance d between one and the other measured from their surfaces. Each ellipsoid can be described by its mass number A_i, charge number Z_i and deformation parameter, β_i.

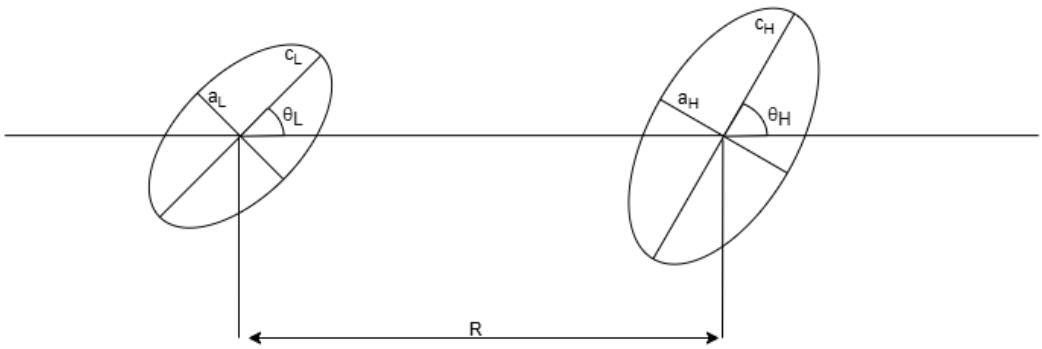

Fig. 2.1: Schematic drawing of the DNS.

Within this model, the deformation parameter is defined as a ratio $\beta_i = c_i/a_i$ between the major c_i, and minor a_i semi-axes respectively. This definition holds up to a limit of $\beta_i \sim 2.1$ which is enough for this current work. This deformation parameter can be linked to the quadrupole deformation by $\beta = \beta_2 + 1.025$ [1, 2] where β_2 is the quadrupole moment. We also can define the semi-axes in respect to the deformation parameter by making use of the volume conservation and the nuclear radius $R_0 = r_0 A^{1/3}$ ($r_0 = 1.16fm$) as:

$$
\begin{aligned}
c_i =& r_{0i} A^{1/3} \beta_i^{2/3} \\
a_i =& r_{0i} A^{1/3} \beta_i^{-1/3}
\end{aligned} \tag{2.1}
$$

2.2.2 Interaction energy

The interaction energy is composed of the Coulomb potential, nuclear potential and rotational energy and in the most general sense has the following form:

$$
\begin{aligned}
V^{int}(A_i, Z_i, \beta_i, \theta_i, R) =& V^C(A_i, Z_i, \beta_L, \beta_H, \theta_L, \theta_H, R) + \\
& V^N(A_i, Z_i, \beta_L, \beta_H, \theta_L, \theta_H, R) + \\
& V^{Rot}(A_i, Z_i, \beta_L, \beta_H, \theta_L, \theta_H, R, l)
\end{aligned} \tag{2.2}
$$

As mentioned previously, the rotational aspect will be ignored in this work. The azimuthal angle can be safely discarded as well, limiting the description of the orientation to be handled by the polar angle θ_i only. Initially a cumbersome function of many variables, some of these variables will disappear in the following sections.

Nuclear interaction

The nuclear potential will be considered as a double folding potential with density dependent nucleon forces of Skyrme-type [3]:

$$
V_N = \int \rho_L(\mathbf{r_L}) \rho_H(\mathbf{R} - \mathbf{r_H}) F(\mathbf{r_L} - \mathbf{r_H}) d\mathbf{r_L} d\mathbf{r_H}. \tag{2.3}
$$

With $\rho_{L,H}$ being the nuclear densities of the light and heavy fragments respectively taken as $\rho = \rho_{00} \frac{1}{1+e^{(r-R)/a}}$ where $a = 0.54fm$ is a diffuseness parameter and $\rho_{00} = 0.17fm^{-3}$ is the saturation density. $F(\mathbf{r_L} - \mathbf{r_H})$ is the effective nucleon-nucleon interaction which is density dependent as well:

$$
F(\mathbf{r_L} - \mathbf{r_H}) = C_0 \left[F_{in} \frac{\rho_L(\mathbf{r_L})}{\rho_{00}} + F_{ex} \left(1 - \frac{\rho_L(\mathbf{r_L})}{\rho_{00}} \right) \right] \delta(\mathbf{r_L} - \mathbf{r_H}). \tag{2.4}
$$

Considering we work with highly individualized fragment nuclei that have small density overlap we have $\rho_0(\mathbf{r}) = \rho_L(\mathbf{r}) + \rho_H(\mathbf{r})$ and it allows us to obtain:

$$F_{in,ex} = f_{in,ex} + f'_{in,ex} \frac{(N_L - Z_H)(N_H - Z_H)}{(N_L + Z_H)(N_H + Z_H)}, \tag{2.5}$$

where we have $C_0 = 300 MeV fm^3$, $f_{in} = 0.09$, $f'_{in} = 0.42$, $f_{ex} = -2.59$, $f'_{ex} = -0.54$.

Coulomb interaction

For the Coulomb part, we start from the approximate formula for the case of two deformed nuclei of arbitrarily orientation given by Ref. [4] but we reach a problem quickly, it become computationally expensive to consider arbitrary orientations between the two fragments. In order to manage this, we consider a slightly different geometry of the system.

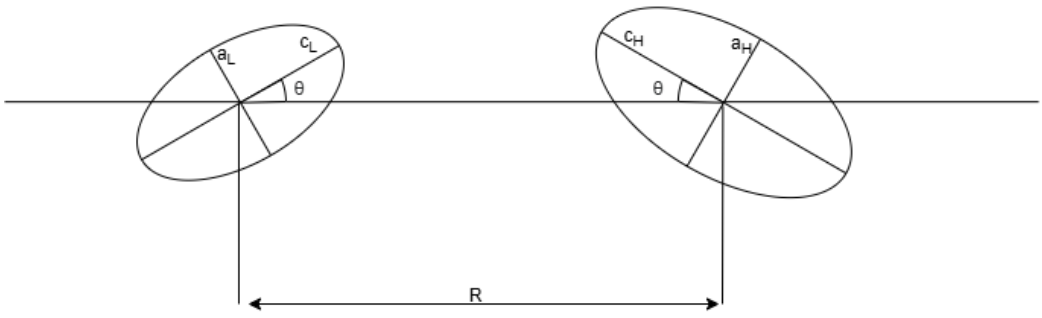

Fig. 2.2: Schematic drawing similar with 2.1 with a different orientation, the fragments share the orientation angle $\theta_L = \theta_H = \theta$

In this arrangement, having $\theta_L = \theta_H = \theta$ we can write the Coulomb interaction in a simplified form:

$$V^C = \frac{e^2 Z_L Z_H}{R} [s(\lambda_L, \theta_L) + s(\lambda_H, \theta_H) - 1 + S(\lambda_L, \lambda_H, \theta)], \tag{2.6}$$

where we consider:

$$\lambda_i^2 = \frac{c_i^2 - a_i^2}{R^2}$$

$$s(\lambda_i, \theta_i) = 3 \sum_{n=0}^{\infty} \frac{P_{2n}(cos\theta_i)}{(2n+1)(2n+3)} \lambda_i^{2n}$$

$$S(\lambda_L, \lambda_H, \theta) = 9 \sum_{j,k=1}^{\infty} \frac{(2j+2k)! P_{2j+2k}(cos\theta)}{(2j+1)(2j+3)(2k+1)(2k+3)(2j!)(2k!)} \lambda_L^{2j} \lambda_H^{2k}. \tag{2.7}$$

Reduction in the degrees of freedom

We return to the interaction potential and look at the disintegration coordinate which is the internuclear distance R. A link between R and d is given by the relation $R = c_L + c_H + d$. We will consider the interaction potential as function of d in the case of ^{106}Mo + ^{146}Ba fragment pair that have no deformation:

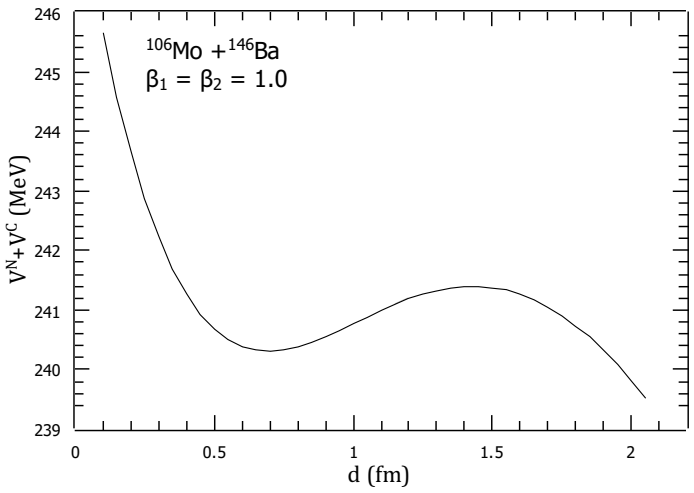

Fig. 2.3: The interaction potential as function of distance between fragments for ^{106}Mo + ^{146}Ba

In Fig. 2.3, we observe two extreme points of interest, a local minimum at $d_m \sim 0.7$ fm which is called the "potential pocket" and a local maximum at $d_B \sim 1.6$ fm. The position of these points is dependent on mass and

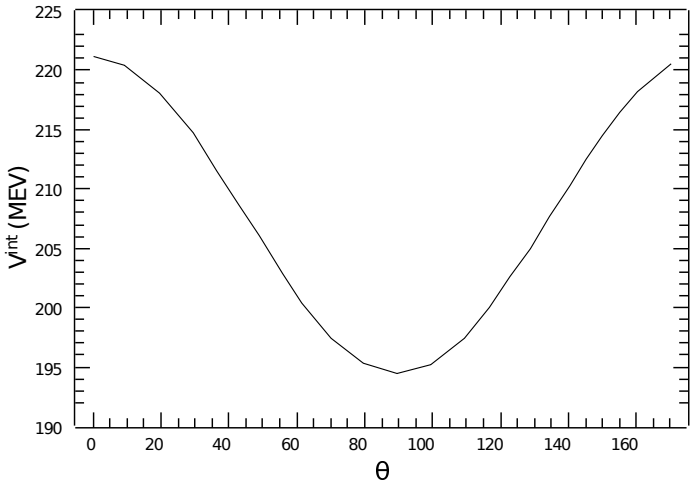

Fig. 2.4: The interaction potential V^{int} as a function of orientation of both fragments $\theta_L = \theta_H = \theta$ for ^{106}Mo + ^{146}Ba. The angle is taken as relative to the vertical Oz axis instead.

charge of the fragments. We can define the "quasi-fission barrier" as the difference between the potential evaluated at d_B and d_m in the following manner $B_{qf} = V^{int}(d_B) - V^{int}(d_m)$. The barrier prevents the system to evolve along the disintegration coordinate and the system gets to remain in the potential pocket long enough that statistical equilibrium is achieved. The statistical equilibrium suggest that the configuration of the system at that position determines the statistical properties of the DNS which is important because all the desired observables of interest can be determined from these properties. As such, and to reduce the number of variables, all calculations will be performed at d_m (R_m).

We turn our attention to the orientation angle now and consider the interaction potential as a function of the orientation of the nuclei in the case of ^{106}Mo + ^{146}Ba fragment pair with $\beta_L = 1.7$, $\beta_H = 1.55$. Both nuclei will turn by the same angle $\theta_L = \theta_H = \theta$ as per the illustration in Fig. 2.2

We observe that a minimum appears at $\theta = 90$ corresponding to a geometry where the fragments are oriented "tip-to-tip". As this orientation seems favorable for minimizing the potential energy, we will consider the system to be in such a geometry in all the following calculations. Also, the number of variables can be reduced from the description of the interaction potential.

2.2.3 Liquid Drop energies

The Liquid Drop Model (LDM) is an attractive model due to its resemblance with the classical liquid drop and its simplicity and is successful at providing a good description for some nuclear properties, of particular interest for us, the binding energies.

This thesis is written with the intent to study and interpret the results for the calculations of some observables of interest: charge distribution, total kinetic energy and neutron multiplicity in the case of radon and radium. This study is done within the context of the di-nuclear system model, an improved scission-point model. There are four Liquid Drop (LD) terms to consider: volume, surface, Coulomb, and symmetry. We will ignore the volume term as it is conserved in our calculations where we will always take the compound nucleus (CN) as a reference point.

Surface energy

We start in a simple manner by considering the energy as being proportional to the surface area $U^{Surf} = \sigma_i S_i$ with σ_i being the surface tension coefficient. We will tackle these two factors one at a time. The surface of a deformed ellipsoid is rather difficult to describe in a neat manner so we will consider it as variation of a spherical nuclei in the following manner $S_i = B_s S_i^0$ with S_i^0 being the surface of a sphere $S_i^0 = 4\pi r_0^2 A_i^{\frac{2}{3}}$ and, if we restrict to axially symmetric nuclei, B_s is a dimensionless parameter taken as:

$$B_S = \frac{1}{2}\eta^{\frac{2}{3}}\left(1 + \frac{\arcsin(\epsilon)}{\eta\epsilon}\right), \tag{2.8}$$

where $\eta = \frac{a}{c}$ is defined as the inverse of the deformation parameter β introduced earlier and $\epsilon = (1-\eta^2)^{1/2}$ is the eccentricity [5].

Returning to the surface tension coefficient, we will introduce a dependence of deformation as a constant σ create a problem where the moments of inertia for the fissioning nuclei get larger than the experimental data [2]. This dependence can be taken:

$$\sigma_i(\beta_i) = \sigma_{0,i}(1 + k_i(\beta_i - \beta_i^{g.s})^2) \tag{2.9}$$

where $\beta_i^{g.s}$ are ground state deformations taken from Ref. [6–8] and $\sigma_{0,i} = 0.9517(1 - 1.7826((N_i - Z_i)^2/A_i^2))$ [9]. For k_i we can introduce a parametrization with dependence of the stiffness of the nucleus C_{vib} given in MeV [10] as:

$$k_i = \frac{1}{1 + \exp[-0.063(C_{vib}(Z_i, A_i) - 67)]}. \tag{2.10}$$

Liquid-Drop Coulomb energy and Symmetry energy

We begin with the uniformly charged sphere with radius R_0 where we consider the Coulomb energy from electrostatics [5] as $U_i^{Coul,0} = \frac{3e^2}{5r_0}\frac{Z_i^2}{A_i^{1/3}}$. We follow the logic used for the surface energy and multiply it by a dimensionless parameter to obtain the energy for a spheroid instead. This parameter takes the following form where η is the inverse of the deformation parameter and ϵ is the eccentricity:

$$B_C = 0.5\frac{\eta^{\frac{2}{3}}}{\epsilon}\ln\left(\frac{1+\epsilon}{1-\epsilon}\right). \tag{2.11}$$

The symmetry energy is taken simply as $U_i^{sym} = 27.612\frac{(N_i - Z_i)^2}{A_i}$

Shell Correction

Per Strutinsky's prescription, we can view the influence of the nucleon shells as a just a small deviation from an otherwise uniform nucleon distribution; the shell correction are given [11] as:

$$\delta U = \sum_\nu E_\nu - \tilde{U}. \tag{2.12}$$

with nucleon energies E_ν and $\tilde{U}$ expressed by the integral $\tilde{U} = \int_{-\infty}^{\tilde{\lambda}} E\tilde{g}(E)dE$. Here we have the uniform distribution function with $\tilde{g}$ and $\tilde{\lambda}$ is a chemical potential taken as [5]

$$\int_{-\infty}^{\tilde{\lambda}} \tilde{g}(E)dE = A. \tag{2.13}$$

2.3 Potential energy surface (PES)

We are ready now to calculate the total potential energy of the system as we have prepared all the necessary ingredients in the following form:

$$\begin{aligned} U(A_i, Z_i, \beta_i, R) = & U_L^{LD}(A_L, Z_L, \beta_L, E^*) + \delta U_L^{shell}(A_L, Z_L, \beta_L, E^*) \\ & + U_H^{LD}(A_H, Z_H, \beta_H, E^*) + \delta U_H^{shell}(A_H, Z_H, \beta_H, E^*) \\ & + V^C(A_i, Z_i, \beta_i, d_m) + V^N(A_i, Z_i, \beta_i, d_m), \end{aligned} \tag{2.14}$$

with the binding energies consisting of the LDM components:

$$U_i^{LD}(A_i, Z_i, \beta_i) = U_i^{surf}(A_i, Z_i, \beta_i) + U_i^C(A_i, Z_i, \beta_i) + U_i^{sym}(A_i, Z_i), \tag{2.15}$$

where δU_i^{shell} is the shell correction for the fragment i. Using Eq. (2.14), we can construct the PES by taking the variation of the deformation parameters β_1 and β_2 for combinations of mass and charge numbers of both fragments in order to obtain a helpful visual depiction of the system's configuration at the scission moment.

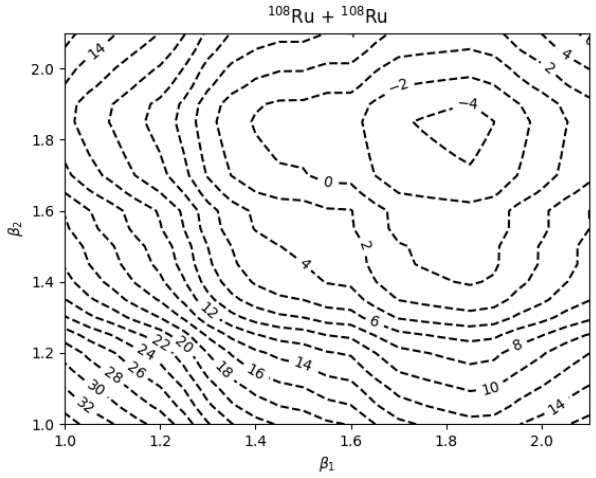

Fig. 2.5: Potential energy surfaces for the DNS ^{108}Ru+^{108}Ru with shell correction. The values are in MeV and are normalized to the energy of the CN

In the PES shown in Fig. 2.5, we see the total energy as decreasing as the system becomes more deformed due to the interaction potential decreasing with deformation while the surface energy increases until a point where an increase in the surface energy part of the LDM compensates the decrease of the interaction potential. This effect is the reason for the minima shown. The minimum's position indicate the most favorable deformations of the fragments at the moment of scission.

2.3.1 Excitation energy and damping

On its way toward fission, the system accumulates a considerable amount of excitation energy due to conservation of energy. This energy impacts the system in a number of ways (e.g neutron emission). Within this model, we have the means to calculate the excitation energy and temperature self-consistently.

We consider the initial excitation energy $E_0^* = E_{n,\gamma} + Q_n$ that the system starts along the fission path with. $E_{n,\gamma}$ is the energy of the incident photon or neutron and Q_n is the reaction heat in case of neutron induced fission. E_0 is zero in case of spontaneous fission and is equal to the γ quanta in the case of electromagnetic induced fission. In order to obtain the entire excitation energy, we must add the difference in potential energies of the initial compound nucleus and the DNS at scission point [12, 13]:

$$\begin{aligned} E^*(A_i, Z_i, \beta_i, d_m) &= E_0^* + Q - V^{int}(\{A_i, Z_i, \beta_i^{g.s}\}, d_m) \\ &- \left[U(\{A_i, Z_i, \beta_i\}, d_m, E^*) - U(\{A_i, Z_i, \beta_i^{g.s}\}, d_m, E^*)\right]. \end{aligned} \tag{2.16}$$

The excitation energy can achieve such high values (~ 20 MeV) that the shell structure is disrupted and we introduced a dependence for excitation energy to the shell correction to account for this.

$$\delta U_i^{shell}(A_i, Z_i, \beta_i, E_i^*) = \delta U_i^{shell}(A_i, Z_i, \beta_i, E_i^* = 0) \exp(-E_i^*/E_D), \tag{2.17}$$

where $E_D = 18.5$ MeV is a damping constant. According to a study [14], the LDM components were found to have a dependency on temperature and so depend on excitation energy as well. We can link the temperature to the excitation energy by using:

$$T = \sqrt{E^*/a}. \tag{2.18}$$

where $a = A/12$ is the density parameter in the Fermi-gas model.

2.4 Statistical model

If we consider the binary decay as a two step process then we can write the total emission probability as a combination of formation probability that would represent the evolution of the system under $U(\{A_i, Z_i, \beta_i\}, d_m)$ until the potential pocket and the decay probability which would represent the system traversing the quasi-fission barrier by having enough excitation energy:

$$\omega(A_i, Z_i, \beta_i, E^*) = \exp\left[-\frac{U(\{A_i, Z_i, \beta_i\}, d_m) + B_{qf}(\{A_i, Z_i, \beta_i\})}{T}\right]. \tag{2.19}$$

2.4.1 Charge and Mass distributions

In order to obtain the charge or mass distributions, we would need to integrate Eq. 2.19 over the PES then perform a summation over mass for charge distribution or over charge for mass distribution:

$$\begin{aligned} Y(A_i) &= N_0 \sum_{Z_i} \int\int d\beta_L d\beta_H \omega(A_i, Z_i, \beta_i, E^*) \\ Y(Z_i) &= N_0 \sum_{A_i} \int\int d\beta_L d\beta_H \omega(A_i, Z_i, \beta_i, E^*) \end{aligned} \tag{2.20}$$

2.4.2 Neutron multiplicity

Shortly post-fission, the nuclear fragments retain excitation energy partitioned to each other in proportion to their masses. In addition to this, these fragments are deformed and, as they relax, they will accumulate deformation energy as well. These energies will determine the fragments to emit

neutrons to reduce their energies. We consider the following description for the emission of both fragments:

$$\begin{aligned}\langle\nu\rangle(Z_i) &= \sum_{A_i,\nu}\int d\beta_1\beta_2\nu P_\nu(A_i,Z_i,\beta_i,E^*)\omega(A_i,Z_i,\beta_i),\\ \langle\nu\rangle(A_i) &= \sum_{Z_i,\nu}\int d\beta_1\beta_2\nu P_\nu(A_i,Z_i,\beta_i,E^*)\omega(A_i,Z_i,\beta_i),\end{aligned} \tag{2.21}$$

and this in the case of emission from a single fragment:

$$\begin{aligned}\langle\nu_i\rangle(Z_i) &= \sum_{A_i,\nu_i}\int d\beta_1\beta_2\nu_i\tilde{P}_{\nu_i}(A_i,Z_i,\beta_i,E^*)\omega(A_i,Z_i,\beta_i),\\ \langle\nu_i\rangle(A_i) &= \sum_{Z_i,\nu_i}\int d\beta_1\beta_2\nu_i\tilde{P}_{\nu_i}(A_i,Z_i,\beta_i,E^*)\omega(A_i,Z_i,\beta_i),\\ \tilde{P}_{\nu_i} &= \int_0^{E^*} d\epsilon_i^* P_C(\epsilon_i^*)P_{\nu_i}(U_i^{def}+\epsilon_i^*).\end{aligned} \tag{2.22}$$

Here, P_ν is the probability that exactly ν neutrons are emitted taken from Jackson formula [15, 16] and P_C is the micro-canonical distribution of the energy partitioned between the two fragments.

2.4.3 Total kinetic energy (TKE)

The total kinetic energy is the entire interaction energy of the system after scission occurs converted into kinetic energy for the fragments. We consider it thus as $TKE = V^C + V^N$ and we can find its distribution with regards to charge as:

$$\langle TKE\rangle(Z_i) = \sum_{A_i}\frac{TKE(A_i,Z_i)Y(A_i,Z_i,E^*)}{Y(A_i,Z_i,E^*)} \tag{2.23}$$

3 Charge distributions and TKE

Having all the necessary tools prepared, we can look into the study of ^{204,206,208}Rn and ^{214,216,218}Ra in the case of electromagnetic-induced fission with $E_0^* = 11$ MeV and the results will be compared with experimental data from Ref. [17]. Some calculations were performed on ^{232,234}U as well to test the reliability of the model.

3.1 Charge distribution

For Rn and Ra, we have obtained symmetric charge distributions ascribed to strong liquid drop effects while U presents asymmetry charge distribution corresponding to a strong shell effect.

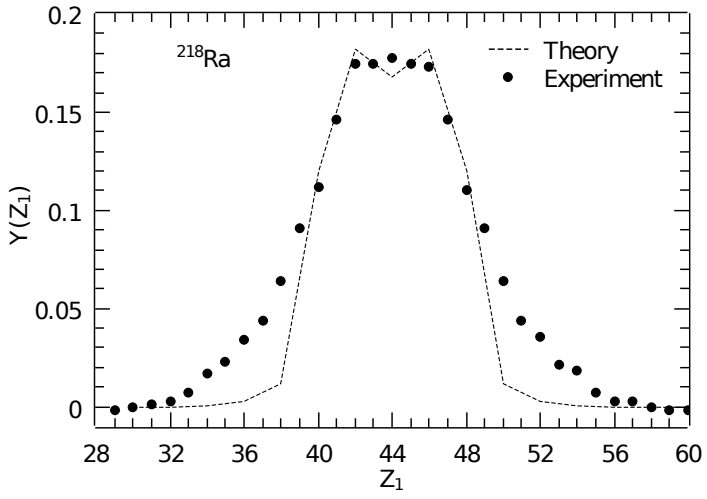

Fig. 3.1: Charge distribution in the case of CN ^{218}Ra

3.2 TKE and supporting distributions

For Rn and Ra, we have obtained mean TKE that feature a plateau at symmetry flanked by two small peaks while U features two asymmetric peaks with a deep valley in between.

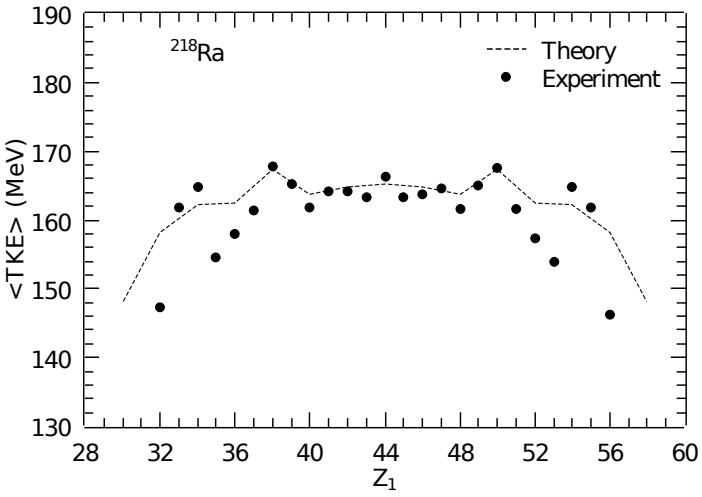

Fig. 3.2: Mean TKE distribution in the case of CN ^{218}Ra

In this chapter, other distributions were calculated and included in other to provide insight as to how other observables change with the increase in charge. We considered in this manner a mean deformation parameter $\langle\beta_i\rangle$, average liquid drop energies $\langle U^{LD}\rangle$, mean shell corrections $\langle\delta U\rangle$ and average excitation energies $\langle E^*\rangle$. All were obtained in a similar manner to $\langle TKE\rangle$

3.3 Discussion

We notice that our calculations reproduce the experimental data very well across the board where experimental data was available. In this section we have correlated all distributions obtained thus far and analyzed particular points, mostly relating to magic numbers such as proton charge number $Z = 50$ but the neutron one appears as well in some configurations that contribute much for some noteworthy points (the pair ^{86}Kr $+^{118}$Sn has, for example, both nuclei as magic nuclei and ^{86}Kr has a magic number of neutrons $N =$

50). Other correlations performed are the peaks in TKE corresponding to minima in deformation and shell correction distributions suggesting that the most stable fragment nuclei have higher interaction potentials [18].

4 Neutron multiplicities

The neutron emission is a process that requires study as the properties of these neutrons give insight in regard to the formation of the fission fragments and partition of the excitation energy between fragments. As such we have studied the number of emitted neutrons from both fragments as well as from a single one.

We have observed that for the isotopes studied we have symmetric neutron multiplicities in the case of considering both fragments. It is considered that this follows the behavior of the excitation energy distribution profile which makes sense on the basis that the fragments with the most energy can emit the largest number of neutrons. We observe that Rn distributions present a plateau like structure at symmetry that is not observed in Ra. Ra distributions have higher peaks than Rn due to having higher excitation energies while having lower neutron separation energies. In the case of single fragment neutron multiplicities we observe a slow increase in the number of emitted neutrons as the nucleus gets heavier as it receives a larger amount of the total excitation energy, followed by an abrupt sawtooth-like drop at $Z_1 = 50$ as for magic nuclei, the neutron separation energies are very large by comparison [19] and thus have lower neutron multiplicities.

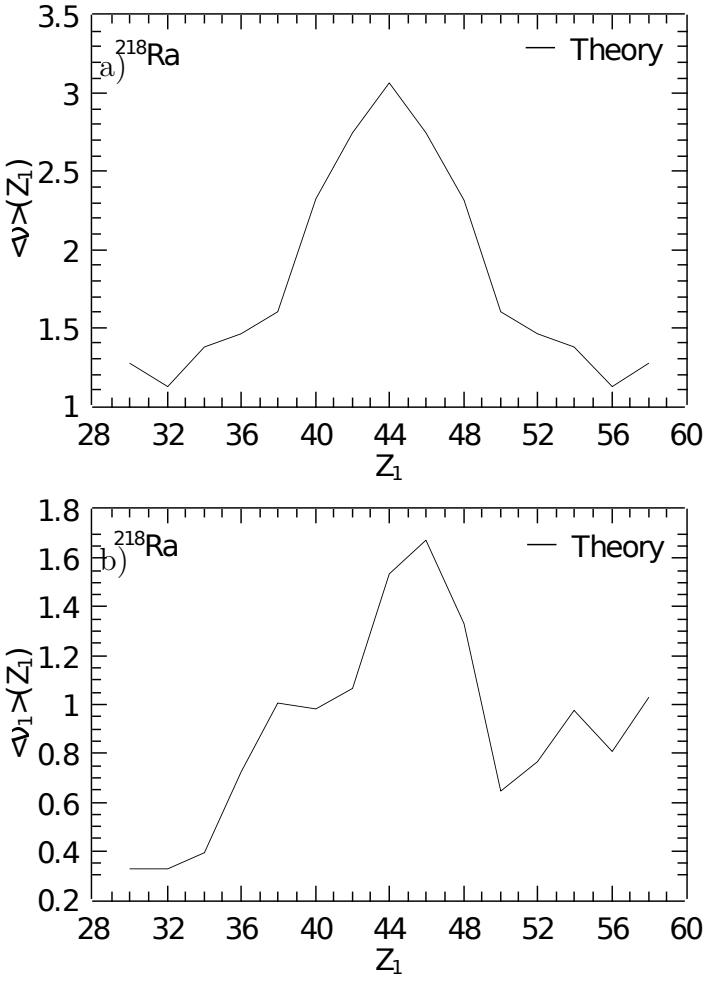

Fig. 4.1: Neutron multiplicities for both fragments (a-top) as well as a single fragment (b-bottom) performed for ^{218}Ra.

5 Conclusions

The model employed was able to provide good description for the charge distributions, total kinetic energy and neutron multiplicity of the fission fragments in the case of electromagnetic induced fission of Rn and Ra isotopes. We have managed to obtain results for these observables of interest and describe very well the experimental data available. We managed to explain the positions of the peaks in charge distributions and the asymmetric peaks in TKE on the basis of magic numbers and in correlation with deformation distribution and shell correction distributions. We explained the neutron multiplicities in a similar manner in relation to the excitation energy distribution and identified the cause for the sawtooth-like drop as the stable magic nuclei that hinder neutron emission. We compared the neutron emission distributions from Rn and Ra and observed slightly different behaviors, for Rn the peaks are roughly at the same value for all isotopes while for Ra, the peaks increase from ^{214}Ra to ^{218}Ra on the basis of increasing excitation energy.

6 Scientific Activity

Published articles

1. Andrei Butuza. “Charge distribution and total kinetic energy in the fission of Rn, Ra and U”. In: The European Physical Journal A 60.11 (Nov. 2024). issn: 1434-601X. doi: 10 . 1140 / epja / s10050 - 024 - 01423- 2. url: http://dx.doi.org/10.1140/epja/s10050- 024- 01423-2.

   Impact factor: 2.6

   AIS: 0.759

2. Andrei Butuza. ”Neutron multiplicity distribution in the fission of Rn and Ra”. accepted for publication In: International Journal of Modern Physics E (2025)

   Impact factor: 1

   AIS: 0.199

Workshops

1. Andrei Butuza. ”Charge, mass and energy distribution of neutron-induced fission of light actinides”. At: 6^{th} Grandmaster Early Career Workshop in Physics GEWP (3-8 September 2023), Cluj Napoca, Romania

Bibliography

[1] Rainer W. Hasse and William D. Myers. *Geometrical Relationships of Macroscopic Nuclear Physics*. ISSN: 0939-1150 Publication Title: Springer Series in Nuclear and Particle Physics. Springer Berlin Heidelberg, 1988. ISBN: 978-3-642-83017-4. DOI: 10.1007/978-3-642-83017-4. URL: http://dx.doi.org/10.1007/978-3-642-83017-4.

[2] Horia Pasca. "Cluster Approach to Fission". PhD thesis. Cluj-Napoca, Romania: Babes-Bolyai University, 2017.

[3] G.G. Adamian et al. "Effective nucleus-nucleus potential for calculation of potential energy of a dinuclear system". In: *International Journal of Modern Physics E* 05.01 (Mar. 1996). Number: 01 Publisher: World Scientific Publishing Co., pp. 191–216. ISSN: 0218-3013. DOI: 10.1142/S0218301396000098. URL: https://doi.org/10.1142/S0218301396000098.

[4] C. Y. Wong. "Interaction Barrier in Charged-Particle Nuclear Reactions". In: *Physical Review Letters* 31.12 (Sept. 1973). Publisher: American Physical Society (APS), pp. 766–769. ISSN: 0031-9007. DOI: 10.1103/physrevlett.31.766. URL: http://dx.doi.org/10.1103/PhysRevLett.31.766.

[5] M. Ivascu and D. N. Poenaru. *Energia de deformare si izomeria formei nucleelor*. Bucuresti: Ed. Academiei Republicii Socialiste Romania, 1981.

[6] Peter Möller and J.Rayford Nix. "Nuclear mass formula with a Yukawa-plus-exponential macroscopic model and a folded-Yukawa single-particle potential". In: *Nuclear Physics A* 361.1 (May 1981). Publisher: Elsevier BV, pp. 117–146. ISSN: 0375-9474. DOI: 10.1016/0375-9474(81)90473-5. URL: http://dx.doi.org/10.1016/0375-9474(81)90473-5.

[7] S. Raman, C.W. Nestor, and P. Tikkanen. "Transition Probability From The Ground To The First-Excited 2+ State Of Even–Even Nuclides". In: *Atomic Data and Nuclear Data Tables* 78.1 (May 2001). Publisher: Elsevier BV, pp. 1–128. ISSN: 0092-640X. DOI: 10.1006/adnd.2001.0858. URL: http://dx.doi.org/10.1006/adnd.2001.0858.

[8] P. Möller and J.R. Nix. "Nuclear masses from a unified macroscopic-microscopic model". In: *Atomic Data and Nuclear Data Tables* 39.2 (July 1988). Publisher: Elsevier BV, pp. 213–223. ISSN: 0092-640X. DOI: 10.1016/0092-640x(88)90022-8. URL: http://dx.doi.org/10.1016/0092-640X(88)90022-8.

[9] W. Greiner, J.Y. Park, and W. Scheid. *Nuclear Molecules*. G - Reference,Information and Interdisciplinary Subjects Series. World Scientific, 1995. ISBN: 978-981-02-1723-5. URL: https://books.google.ro/books?id=ZDFqDQAAQBAJ.

[10] Walter Greiner and Joachim A. Maruhn. *Nuclear Models*. Springer Berlin Heidelberg, 1996. ISBN: 978-3-642-60970-1. DOI: 10.1007/978-3-642-60970-1. URL: http://dx.doi.org/10.1007/978-3-642-60970-1.

[11] M. Brack et al. "Funny Hills: The Shell-Correction Approach to Nuclear Shell Effects and Its Applications to the Fission Process". In: *Reviews of Modern Physics* 44.2 (Apr. 1972). Publisher: American Physical Society (APS), pp. 320–405. ISSN: 0034-6861. DOI: 10.1103/revmodphys.44.320. URL: http://dx.doi.org/10.1103/RevModPhys.44.320.

[12] A. V. Andreev et al. "Possible explanation of fine structures in mass-energy distribution of fission fragments". In: *The European Physical Journal A* 22.1 (Oct. 2004). Number: 1 Publisher: Springer Science and Business Media LLC, pp. 51–60. ISSN: 1434-601X. DOI: 10.1140/epja/i2004-10017-9. URL: http://dx.doi.org/10.1140/epja/i2004-10017-9.

[13] A. V. Andreev, G. G. Adamian, N. V. Antonenko, and S. P. Ivanova. "Bimodality and charge splitting in fission of actinides". In: *The European Physical Journal A* 26.3 (Dec. 2005). Number: 3 Publisher: Springer Science and Business Media LLC, pp. 327–332. ISSN: 1434-601X. DOI: 10.1140/epja/i2005-10179-x. URL: http://dx.doi.org/10.1140/epja/i2005-10179-x.

[14] G. Sauer, H. Chandra, and U. Mosel. "Thermal properties of nuclei". In: *Nuclear Physics A* 264.2 (June 1976). Number: 2 Publisher: Elsevier BV, pp. 221–243. ISSN: 0375-9474. DOI: 10.1016/0375-9474(76)90429-2. URL: http://dx.doi.org/10.1016/0375-9474(76)90429-2.

[15] J.R. Huizenga. *Studies of nuclear fission, low-energy nuclear reactions and transuranic nuclei. Progress report, June 1, 1972–June 1, 1973*. Tech. rep. Rochester Univ., NY (USA). Dept. of Chemistry, 1973.

[16] H. Paşca, A. V. Andreev, G. G. Adamian, and N. V. Antonenko. "Influence of the transition from symmetric to asymmetric fission mode on the average total kinetic energy and neutron multiplicity". In: *Physical Review C* 108.1 (July 2023). ISSN: 2469-9993. DOI: 10.1103/physrevc.108.014613. URL: http://dx.doi.org/10.1103/PhysRevC.108.014613.

[17] K-H Schmidt et al. "Relativistic radioactive beams: A new access to nuclear-fission studies". en. In: *Nucl. Phys. A* 665.3-4 (Feb. 2000). Number: 3-4 Publisher: Elsevier BV, pp. 221–267.

[18] Andrei Butuza. "Charge distribution and total kinetic energy in the fission of Rn, Ra and U". In: *The European Physical Journal A* 60.221 (Nov. 2024). ISSN: 1434-601X. DOI: 10.1140/epja/s10050-024-01423-2. URL: http://dx.doi.org/10.1140/epja/s10050-024-01423-2.

[19] Meng Wang et al. "The AME2016 atomic mass evaluation (II). Tables, graphs and references". In: *Chinese Physics C* 41.3 (Mar. 2017), p. 030003. ISSN: 1674-1137. DOI: 10.1088/1674-1137/41/3/030003. URL: http://dx.doi.org/10.1088/1674-1137/41/3/030003.